Nuclear-spin-lattice relaxation-rate measurements in $YBa_2Cu_3O_7$

J. A. Martindale, S. E. Barrett, D. J. Durand, K. E. O'Hara, C. P. Slichter,* W. C. Lee, and D. M. Ginsberg
Department of Physics and Frederick Seitz Materials Research Laboratory, University of Illinois at Urbana-Champaign, 1110 West Green Street, Urbana, Illinois 61801-3080
(Received 25 July 1994)

Experimental details are given for NMR and NQR measurements of nuclear-spin-lattice relaxation rates for the planar copper and oxygen sites in $YBa_2Cu_3O_7$. Enrichment of samples with ^{17}O, alignment of powder samples, elimination of artifacts in relaxation-rate measurements, and the unusual aspects of weak magnetic-field experiments used to overcome an observed magnetic-field dependence in the rates are described. The role of fluxoids in the magnetic-field dependence of the relaxation rates is discussed. The relaxation rate data are shown to be inconsistent with a spin-singlet, orbital *s*-wave pairing state with an isotropic energy gap.

I. INTRODUCTION

Nuclear-spin-lattice relaxation rates W_1 represent one means of learning about the electronic properties of superconductors. Measurement of W_1 in ^{27}Al revealed the presence of the coherence peak just below T_c,[1,2] which provided early support for the BCS theory of superconductivity.[3] Since that time, the measurement of W_1 in superconductors has been utilized to obtain such information as the size of the energy gap,[2,4] anisotropy of the energy gap,[4] and the possibility of unconventional (i.e., nonorbital *s*-wave) pairing states.[5] One therefore ought to expect NMR measurements in the high-T_c superconductors of such quantities as W_1 to provide useful information about the superconducting-state properties of these materials.

There are, however, many potential obstacles to obtaining reliable measurements of W_1 in the superconducting state. For example, measurements of W_1 in type-I superconductors often required field-cycling techniques to overcome the exclusion of the magnetic field in the superconducting state.[1] Experiments in type-II superconductors do not suffer from this problem, but other difficulties may occur, such as a magnetic-field dependence for the relaxation rate.[4] In the high-T_c superconductors, several difficulties arise in obtaining reliable W_1 data. The anisotropy of these materials provides one example: one needs well-aligned samples in order to be able to study the anisotropy of quantities such as W_1.

We have published several short papers in which we reported data for spin-lattice relaxation rates in $YBa_2Cu_3O_7$.[6-8] Due to the brief nature of these papers, many experimental details had to be excluded. We now want to describe in more depth some of the experimental procedures and techniques we have made use of in our W_1 measurements. This work is organized as follows. We describe the experimental details in Sec. II. This section covers such topics as ^{17}O enrichment, sample alignment, methods used to remove artifacts from W_1 measurements, and the unusual aspects of our weak-field experiments. Section III presents some new aspects of our measurements, emphasizing potential explanations for the field dependence observed for the spin-lattice relaxation rates for the planar copper and oxygen nuclei in the superconducting state. In Sec. IV, we discuss the nature of the pairing state in $YBa_2Cu_3O_7$ and the potential that the NMR data have for yielding information about the spin and orbital pairing.

II. EXPERIMENT

We have utilized both single crystals and powders in our experiments. The preparation of these samples has been described in detail elsewhere,[9-11] so we shall focus here on their manipulation for our NMR experiments. We note that all of the samples, with the exception of the ^{17}O-enriched samples, showed excellent superconducting transitions: $T_c = 93$ K in zero field with narrow transitions and 100% shielding fractions as determined by SQUID measurements and the change in inductance of a NQR coil. The samples enriched in ^{17}O exhibited broader transitions with approximately 80% shielding; $T_c = 92.5$ K in zero field. The ^{17}O-enriched samples also had broader $^{63}Cu(2)$ NQR lines, indicative of samples which are slightly oxygen deficient;[12,13] we estimate the oxygen content of these samples to be ≥ 6.95. Nonetheless, all of the static and dynamic ^{63}Cu and ^{17}O NMR properties of these latter samples agreed with previous measurements.

As mentioned above, we enriched some of our powder samples with ^{17}O. This was necessary because the only isotope of oxygen with a spin is ^{17}O ($I = \frac{5}{2}$), whose natural abundance is very low, 0.037%. The enrichment procedure was as follows. The $YBa_2Cu_3O_7$ powder (1.15 g) was placed in a platinum boat in the exchange apparatus. The exchange apparatus, which is described in more detail elsewhere,[14,15] was enclosed and consisted of brass and quartz tubing with a total volume of approximately 0.25 l and a pump to circulate the gas in the apparatus. The treatment cycle began with the powder being heated from room temperature to 675 °C at 85 °C/h under vacuum. The powder was held under vacuum at 675 °C for 14

h. The oxygen gas (0.25 l, 1 atm, ~45 at. % ^{17}O) was then added; during the remainder of the process, the oxygen gas was circulated continuously through the system which included a cold trap to remove water or other impurities. The powder was heated to 925 °C at 100 °C/h and held at that temperature for 24 h. The powder was then cooled at 12 °C/h to 425 °C. After holding at 425 °C for 25 h, the powder was removed from the apparatus immediately to quickly bring it to room temperature. As previously stated, powders which underwent this procedure showed signs of being slightly oxygen deficient but had NMR properties, such as shifts and relaxation rates, which were consistent with fully oxygenated samples.

For both powders and single crystals, alignment of the samples was necessary to obtain reliable information about the anisotropy of the relaxation rates. The alignment of the single-crystal sample has been described previously,[11] so we turn our attention here to the alignment of powder samples. Our procedure followed the method of Farrell *et al.*,[16] in which the powder was mixed with epoxy, and this mixture was placed in a magnetic field. The alignment of the *c* axes of the powder particles along the direction of the magnetic field was frozen in place when the epoxy hardened. We used powder which passed through a number-635 sieve (particle size <20 μm). In studying the effect of packing fraction (defined to be the percent by volume of the powder-epoxy mixture which is powder) on alignment, we found that the alignment [as determined by the linewidth of the ^{63}Cu(2)$+\frac{1}{2}\leftrightarrow-\frac{1}{2}$ transition with $\mathbf{H}_0\|\mathbf{c}$] was as good as for single crystals for packing fractions of 25% or less. We have also found that the viscosity of the epoxy [Stycast 1266 (Emerson and Cuming, Woburn, MA)] has a large impact on sample alignment: samples made with epoxy immediately after the epoxy was mixed (when the epoxy was not very viscous) exhibited settling of the powder particles which interfered with the alignment. For our procedure, we let the epoxy harden somewhat before mixing with the powder; waiting 1–2 h (depending on the age of the starting materials) yielded epoxy which had the proper viscosity (roughly the viscosity of glycerol). The powder (<20 μm) and epoxy (viscosity of glycerol) were mixed in the proper ratio (packing fraction $\leq 25\%$) and placed in a sample holder. The sample holder was made from a cast of the same epoxy (Stycast 1266) and consisted of accurately machined square blocks (for accurate alignment of the sample for experiments with either $\mathbf{H}_0\|\mathbf{c}$ or $\mathbf{H}_0\perp\mathbf{c}$) with a hollow cylindrical region in between into which the powder-epoxy mixture was poured. The sample holder was mounted on a plexiglass stand in the probe used for the NMR measurements, and the probe was placed in a magnetic field ($H_0\sim 8$ T) for the alignment-hardening process. Following this procedure yielded *c*-axis alignment of the powder as good as for single crystals as demonstrated in Fig. 1.

Our measurements of W_1 were obtained utilizing a homebuilt pulse spectrometer employing quadrature detection and by using inversion recovery. Signals were obtained by integrating the spin echo gotten from the pulse sequence π-t_d-$\pi/2$-τ-π-τ-echo. We made use of the phase cycling in the pulse sequence, both for the inversion pulse and for the echo sequence, in order to remove the effects of stimulated echoes[17,18] as well as to improve detection of small signals.[19] The spectrometer allowed us to minimize the effects of drift in the apparatus, which could have posed a significant problem because some of our measurements required many hours of signal averaging. This was accomplished by obtaining one echo for one set of phases of the pulses in the phase cycling sequence for each of eight values of t_d and digitally storing the data using DSP Technology, Inc. (Fremont, CA) model 2860 or model 2824 digitizers with model 4101 averagers. The spectrometer then obtained an echo for each of the eight values of t_d for the next set of pulse phases, again storing the data. By cycling through the sequence in this manner, we obtained eight points for the magnetization recovery curve which were free of the effects of apparatus drift. The data were fitted by a least-squares procedure to the appropriate magnetization recovery curve; error bars for the resulting W_1 were determined from the condition $\Delta\chi^2=1$. The nuclear magnetization M after a time t_d following an inversion pulse will in general have a multiexpotential recovery for $I>1/2$.[20] For ^{63}Cu, which has $I=\frac{3}{2}$, the recovery of the $+\frac{1}{2}\leftrightarrow-\frac{1}{2}$ transition following inversion of these two levels in the presence of quadrupole splittings is given by

$$M(t_d)=M(t_d=\infty)\times[1-2(\tfrac{1}{10}e^{-2W_1t_d/3)}+\tfrac{9}{10}e^{-4W_1t_d})]\ . \quad (1)$$

Here W_1 is defined to be the transition rate between the $|m|=\frac{3}{2}$ and $|m|=\frac{1}{2}$ levels. For ^{17}O with $I=\frac{5}{2}$, following inversion of the $\pm\frac{1}{2}\leftrightarrow\pm\frac{3}{2}$ transition, the recovery of the magnetization will be given by

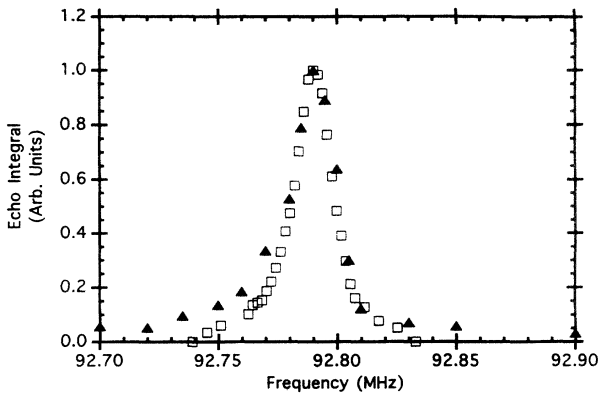

FIG. 1. Comparison of line shapes for the ^{63}Cu(2)$+\frac{1}{2}\leftrightarrow-\frac{1}{2}$ transition with $\mathbf{H}_0\|\mathbf{c}$ ($H_0=8.12$ T) at $T=295$ K for a single-crystal sample (□) and for an aligned powder sample (□). Although the linewidths (FWHM) for these two samples agree, the aligned powder sample shows signal intensity at higher and lower frequencies where the single-crystal sample shows none.

$$M(t_d)=M(t_d=\infty)[1-2(\tfrac{1}{35}e^{-2W_1t_d/3}+\tfrac{3}{56}e^{-2W_1t_d}+\tfrac{1}{40}e^{-4W_1t_d}+\tfrac{25}{56}e^{-20W_1t_d/3}+\tfrac{25}{56}e^{-10W_1t_d})] . \quad (2)$$

In this case, $W_1=\frac{3}{5}W_{5/2\leftrightarrow 3/2}$, consistent with the convention established by Millis, Monien, and Pines.[21] It is these quantities W_1 obtained by fitting the experimental data to the appropriate recovery form which are reported in our previous publications and in Sec. III.

The data in Fig. 1 show that this aligned powder sample has significant signal intensity at higher and lower frequencies where the single crystal has none. This "baseline" was found in all of our aligned powder samples and is believed to be from other nearby resonance lines due to grossly misaligned particles. Although most of the powder particles are well aligned (as revealed by the agreement of the linewidth with that for the single-crystal sample), some could not be. Electron micrographs revealed particles which appeared to be two crystallites grown together. These particles would not have a unique direction for their c axis and so could not align along the magnetic field during the alignment procedure, leading to a powder pattern contribution from these crystallites. Thus, the spectrum shown in Fig. 1 for the aligned powder sample consists of the single-crystal-like line for the ^{63}Cu(2)$+\frac{1}{2}\leftrightarrow-\frac{1}{2}$ transition of well-aligned particles superimposed on a relatively flat background due to misaligned powder particles The baseline created difficulties for W_1 measurements: the baseline extends under the peak of the line and has a different W_1 and T_2. The problem was manifested as W_1 values which depended on the pulse separation time τ in the echo sequence, in W_1 values which did not agree with the single-crystal results or NQR measurements, and by relatively poor fits to the theoretical magnetization recovery curves; see Fig. 2.[14] The baseline problem was most severe for the ^{63}Cu(2)$+\frac{1}{2}\leftrightarrow-\frac{1}{2}$ transition (both $\mathbf{H}_0\|\mathbf{c}$ and $\mathbf{H}_0\perp\mathbf{c}$) for strong magnetic fields ($H_0\geq 4.14$ T) but also occurred for the ^{17}O(2,3) for all transitions. The ^{63}Cu(2)$\pm\frac{3}{2}\leftrightarrow\pm\frac{1}{2}$ transitions with $\mathbf{H}_0\|\mathbf{c}$ showed no effect of a baseline, presumably because they are far removed from any other lines.

Our solution to the baseline problem took two forms: (1) perform measurements on transitions unaffected by the baseline, or (2) subtract off the baseline contribution. Solution (1) was used for strong-field measurements of $^{63}W_{1c}$ ($^{\eta}W_{1\alpha}$:η labels the nucleus, α indicates the spin quantization axes) for the planar copper nuclei, since as mentioned above, the $\pm\frac{3}{2}\leftrightarrow\pm\frac{1}{2}$ transitions showed no effect of a baseline. Solution (2) was used for strong-field ($H_0\geq 4.14$ T) measurements of $^{63}W_{1c}$ and $^{63}W_{1a}$ using the $+\frac{1}{2}\leftrightarrow-\frac{1}{2}$ transition as well as for strong-field ($H_0\geq 4.14$ T) measurements of $^{17}W_{1c}$ (both the $-\frac{1}{2}\leftrightarrow-\frac{3}{2}$ and $-\frac{3}{2}\leftrightarrow-\frac{5}{2}$ transitions). For $H_0\leq 0.67$ T, data for both copper and oxygen showed no significant baseline contribution. The baseline subtraction method used two sets of magnetization recovery data which had the same eight values of t_d. One recovery curve was measured on the peak of the line, and the other was measured at a nearby point on the baseline. Either the higher- or lower-frequency baseline could be used since the result obtained was the same. The baseline data were then subtracted from the peak data and this difference fitted to the theoretical magnetization recovery curve. Figure 3 shows the effect of the baseline subtraction: the data fit the recovery curve quite well, and the value of W_1 thus obtained agrees within error bars with other measurements. This method worked provided one chose times t_d which yielded values of $[M(t_d=\infty)-M(t_d)]/2M(t_d=\infty)$ which were not too small: $\gtrsim\frac{1}{3}$ for ^{63}Cu(2), $\gtrsim\frac{1}{30}$ for

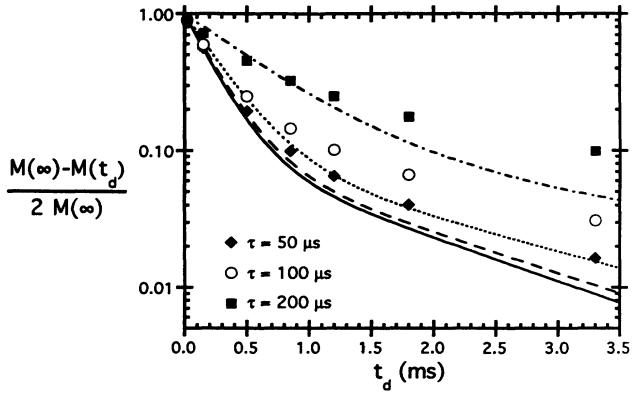

FIG. 2. Magnetization recovery data demonstrating the influence of the baseline. These data were taken on the ^{63}Cu(2)$+\frac{1}{2}\leftrightarrow-\frac{1}{2}$ transition with $\mathbf{H}_0\|\mathbf{c}$ ($H_0=8.12$ T) at $T=101$ K. The symbols show data for different times τ between the $\pi/2$ and π pulses in the echo sequence: $\tau=50$ μs (♦), $\tau=100$ μs (○), and $\tau=200$ μs (■). The dashed line ($\tau=50$ μs), dotted line ($\tau=100$ μs), and dash-dotted line ($\tau=200$ μs) are the fits to the experimental data, and the solid line is the expected recovery curve based upon the value of $^{63}W_{1c}$ obtained by NQR (for which no baseline exists).

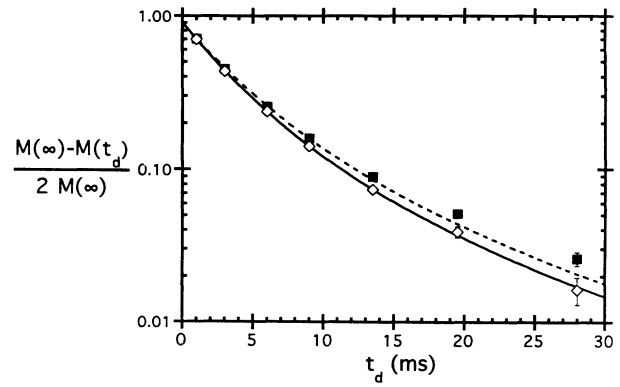

FIG. 3. Magnetization recovery curves for the ^{17}O(2,3) sites for the $-\frac{3}{2}\leftrightarrow-\frac{5}{2}$ transition with $\mathbf{H}_0\|\mathbf{c}$ ($H_0=8.30$ T) at $T=100$ K, illustrating the baseline correction technique. The solid symbols are the peak data, and the open symbols are the baseline data subtracted from the peak data. The fits to the theoretical recovery curve are given by the dashed line for the peak data and by the solid line for the baseline-corrected data. The fit to the baseline-corrected data is better as well as yielding a value of $^{17}W_{1c}$ in agreement with other measurements.

^{17}O(2,3) (depending on temperature and separation time τ in the echo sequence).

We now turn to a discussion of the weak-field experiments. The need for weak-field measurements arises because the relaxation rates for both ^{63}Cu(2) and ^{17}O(2,3) depend on magnetic-field strength in the superconducting state.[7,8,22,23] Theories of W_1 in the superconducting state ordinarily apply only to the case of zero applied field. The observation of a field dependence for W_1 therefore requires zero-field-limit data for comparison with theory. One can actually measure $^{63}W_{1c}$ in zero field by nuclear quadrupole resonance (NQR). However, to get $^{63}W_{1a}$ and $^{17}W_{1c}$, one must apply a magnetic field. Evidence that the magnetic fields utilized in our measurements of $^{63}W_{1a}$ ($H_0=0.45$ T) and $^{17}W_{1c}$ ($H_0=0.67$ T) were sufficiently weak is that $^{63}W_{1c}$ obtained with $H_0=0.67$ T was identical within experimental error with the zero-field NQR result.

Using weak magnetic fields, however, created experimental conditions atypical of most NMR experiments. Let us begin with the general nuclear spin Hamiltonian (ignoring spin-spin couplings):[24]

$$\mathcal{H}=-\hbar\gamma_n\mathbf{H}_0(\underline{\mathbf{1}}+\underline{\mathbf{K}})I + \frac{eQ}{4I(2I-1)}\{V_{zz}(3I_z^2-I^2)+(V_{xx}-V_{yy})(I_x^2-I_y^2)\}\ , \tag{3}$$

where γ_n is the nuclear gyromagnetic ratio, $\underline{\mathbf{K}}$ is the magnetic shift tensor consisting of the chemical (orbital) and Knight (spin) shifts, I is the nuclear spin operator, e is the electron charge, Q is the nuclear electric quadrupole moment (for $I>\frac{1}{2}$), and $V_{\alpha\alpha}$ are the diagonal elements of the electric-field gradient (EFG) tensor. In typical NMR experiments, either the Zeeman term or the quadrupole term in Eq. (3) will be dominant, with the other either ignorable or treatable as a perturbation. In our weak-field measurements of $^{63}W_{1a}$ and $^{17}W_{1c}$, neither the Zeeman interaction nor the quadrupole interaction was large enough to dominate the other.

We will examine the situation for the ^{63}Cu(2) nuclei first. As mentioned above, one can measure $^{63}W_{1c}$ in zero field by NQR. For the ^{63}Cu(2) site the EFG tensor is axially symmetric about the c axis;[25] in zero magnetic field the Hamiltonian is $\mathcal{H}=e^{63}Q^{63}V_{zz}(3I_z^2-I^2)/12$, where $z=c$ (and recalling $^{63}I=\frac{3}{2}$). The eigenstates are the eigenstates of I_z and are shown on the left in Fig. 4. If we now apply a magnetic field perpendicular to the c axis, the Hamiltonian is

$$\mathcal{H}=-\hbar^{63}\gamma_n H_0(1+{}^{63}K_{aa})I_x+\tfrac{1}{12}e^{63}Q^{63}V_{zz}(3I_z^2-I^2)\ . \tag{4}$$

For the planar copper site the a and b directions are indistinguishable, so $^{63}K_{aa}=^{63}K_{bb}$. If we treat the Zeeman term as a perturbation, we get the energy levels (to first order) shown on the right in Fig. 4.

We want to measure $^{63}W_{1a}$. By $^{63}W_{1a}$ and $^{63}W_{1c}$, we mean the rates given by

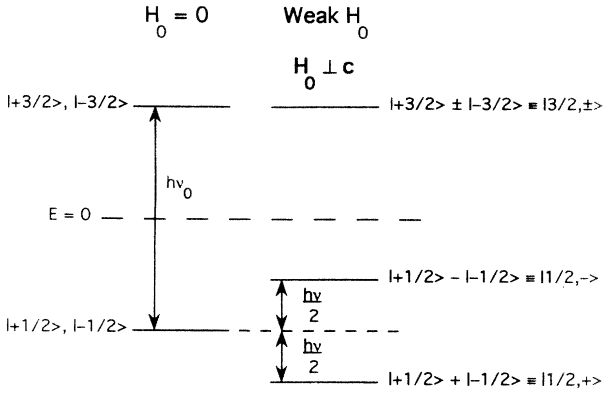

FIG. 4. Energy level diagram for the ^{63}Cu(2) nuclei in zero magnetic field (left) and with a weak magnetic field applied perpendicular to the c axis (right). The states $|m\rangle$ are eigenstates of $I_z=I_c$. The frequency ν_0 (approximately 31.5 MHz) is defined to be $\nu_0=(e^{63}Q^{63}V_{zz})/(2h)$, and ν (10.0 MHz for $H_0=0.45$ T) is given by $\nu={}^{63}\gamma_n H_0(1+{}^{63}K_{aa})/\pi$.

$$^{63}W_{1a}=\tfrac{3}{2}\hbar^2[\overline{h_b^2}(^{63}\omega_0)+\overline{h_c^2}(^{63}\omega_0)]^{63}\gamma_n^2\tau\ , \tag{5}$$

$$^{63}W_{1c}=\tfrac{3}{2}\hbar^2[\overline{h_a^2}(^{63}\omega_0)+\overline{h_b^2}(^{63}\omega_0)]^{63}\gamma_n^2\tau\ , \tag{6}$$

where $\overline{h_\alpha^2}(\omega_0)$ is the mean-square value of the α component of the fluctuating magnetic hyperfine fields responsible for the relaxation at the nuclear resonance frequency ω_0, and τ is the correlation time (assumed isotropic). For the ^{63}Cu(2) nuclei, $\overline{h_a^2}=\overline{h_b^2}$, and therefore $^{63}W_{1a}=^{63}W_{1b}$. Figure 5 shows the energy levels and wave functions along with those components of the hyperfine field which can induce transitions between the levels. To measure $^{63}W_{1a}$ in an experiment, one needs to monitor the magnetization recovery for two levels connected by the c component of the hyperfine fields since $\overline{h_a^2}=\overline{h_b^2}$ occurs in both $^{63}W_{1a}$ and $^{63}W_{1c}$, and $\overline{h_c^2}$ contributes only to $^{63}W_{1a}$. There are two possibilities: $|\frac{1}{2},+\rangle\leftrightarrow|\frac{1}{2},-\rangle$ or $|\frac{3}{2},+\rangle\leftrightarrow|\frac{3}{2},-\rangle$. The transition between $|\frac{1}{2},+\rangle$ and $|\frac{1}{2},-\rangle$ is the only practical one because the $|\frac{3}{2},+\rangle\leftrightarrow|\frac{3}{2},-\rangle$ resonance frequency would be

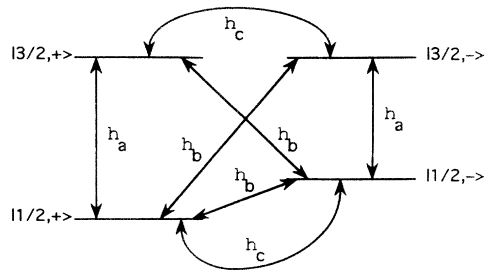

FIG. 5. The energy levels for the ^{63}Cu(2) nuclei in the presence of a weak magnetic field applied perpendicular to the c axis (as in Fig. 4) shown with the components of the magnetic hyperfine fields which can cause transitions between the levels and which can therefore give rise to spin-lattice relaxation.

far too low for a weak-field experiment. With $H_0=0.45$ T, the $|\frac{1}{2},+\rangle \leftrightarrow |\frac{1}{2},-\rangle$ transition occurs at 10.0 MHz. The relaxation modes may be found to be $2W_{1c}$, $-2W_{1c}+6W_{1a}$, and $2W_{1c}+(\frac{2}{3})W_{1a}$. For a measurement between $|\frac{1}{2},+\rangle$ and $|\frac{1}{2},-\rangle$, one finds the recovery should be single exponential with the rate given by $2W_{1c}+(\frac{2}{3})W_{1a}$.

For $H_0=0.45$ T, however, perturbation theory fails to predict the form of the magnetization recovery accurately. One must therefore diagonalize the Hamiltonian of Eq. (4) exactly and calculate the relaxation modes numerically. Because $I=\frac{3}{2}$, one expects that in general the magnetization recovery after an inversion pulse may involve three exponentials:[20]

$$M(t_d)=M(t_d=\infty)\left[1-2\sum_{k=1}^{3} c_k e^{-r_k t_d}\right] . \quad (7)$$

Here c_k and r_k depend on $^{63}W_{1a}$ and $^{63}W_{1c}$. One finds that c_k depends only on the ratio $^{63}W_{1a}/^{63}W_{1c}$; r_k depends on both $^{63}W_{1a}/^{63}W_{1c}$ and $^{63}W_{1c}$, being directly proportional to $^{63}W_{1c}$. Figures 6 and 7 show the dependences of c_k and r_k on $^{63}W_{1a}/^{63}W_{1c}$. By using $^{63}W_{1c}$ measured by NQR on the same sample, and by making use of the information in Figs. 6 and 7, we were able to fit the magnetization recovery data to Eq. (7) to extract $^{63}W_{1a}/^{63}W_{1c}$ and therefore $^{63}W_{1a}$.

A similar situation occurred in the $^{17}W_{1c}$ measurement in weak field. In that experiment, $H_0=0.67$ T was applied parallel to the c axis. The ^{17}O(2,3) EFG tensor, unlike the ^{63}Cu(2), is not symmetric about the c axis: it is nearly axially symmetric about the Cu-O-Cu bond axis.[26,27] Because of the symmetry of the EFG tensor and the orientation and strength of the applied magnetic field, we again had to use numerical methods to diagonalize the Hamiltonian and to determine the form of the magnetization recovery curves. We took $^{17}W_{1,\parallel}=0.61\,^{17}W_{1c}$ and $^{17}W_{1,\perp}=1.09\,^{17}W_{1c}$ (determined by direct measurement of the relaxation rates[6,28] as well as by Knight shift data[27,29]); $\parallel$ means H_0 parallel to the Cu-O-Cu bond axis, and $\perp$ means H_0 in the ab plane but perpendicular to the Cu-O-Cu bond axis. We observed the transition occurring at ≈ 4.3 MHz between states which were approximately $m_c=-\frac{1}{2}$ and $m_c=-\frac{3}{2}$. These data ought to be free of magnetic-field effects: $^{63}W_{1c}$ measured with $H_0=0.67$ T, $\mathbf{H_0}\|\mathbf{c}$ yielded the same result as zero-field NQR measurements in the same sample.

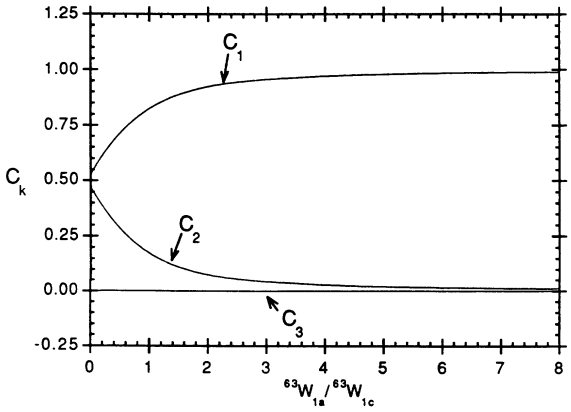

FIG. 6. Dependence of c_k from Eq. (7) on the ratio $^{63}W_{1a}/^{63}W_{1c}$.

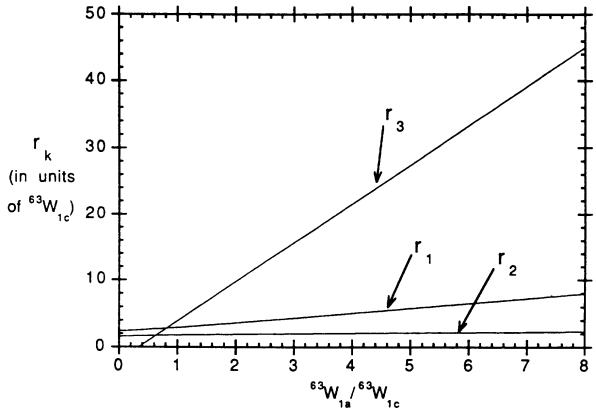

FIG. 7. Dependence of r_k from Eq. (7) on the ratio $^{63}W_{1a}/^{63}W_{1c}$ after dividing out the dependence of r_k on $^{63}W_{1c}$.

III. DATA

Since we have previously published the results of the experiments, we shall just touch briefly on some aspects we have not previously mentioned. Figure 8 shows data measured on a single sample at 0.67 and 8.30 T with the magnetic field along the c axis for both ^{63}Cu and ^{17}O. These data demonstrate that both $^{63}W_{1c}$ and $^{17}W_{1c}$ depend on magnetic-field strength in the superconducting state; we have reported previously that $^{63}W_{1a}$ is less

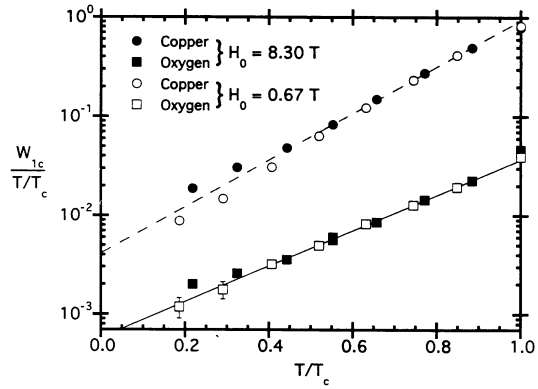

FIG. 8. W_{1c} divided by T/T_c vs T/T_c for copper (circles) and oxygen (squares) for field strengths of 8.30 T (solid symbols) and 0.67 T (open symbols). The dashed and solid lines are fits to the functional form $W_{1c}/(T/T_c)=A\exp[B(T/T_c)]$ for the high-temperature data for the copper and the oxygen, respectively. These show that the copper and the oxygen relaxation rates are independent of field strength in the higher-temperature region, but that both become field dependent at low temperature.

dependent on field strength.[7] In the normal state, we have observed all rates to be independent of magnetic field strength. As mentioned in Sec. I, field-dependent relaxation rates have been observed in other type-II superconductors.[4] In some cases, such as ^1H relaxation rates in $V_{0.46}Ti_{0.31}H_{0.23}$ (Ref. 30) and in κ-$(ET)_2Cu[N(CN)_2]Br$,[31] the mechanism has been shown to arise from fluxoids. Recently, Corey in our laboratory has shown that fluxoids explain the field dependence of $^{63}W_{1c}$ in $YBa_2Cu_3O_7$.[32]

The data in Fig. 8 show that the effect of fluxoids is different for the planar copper and for the planar oxygen. Once the effect of field strength on T_c is removed by using the reduced temperature T/T_c, the data for both copper and oxygen are field independent from T_c down to a certain value of T/T_c, below which the strong-field and weak-field data separate. This divergence occurs at different values of T/T_c for copper and for oxygen: copper at $T/T_c \cong 0.55$ and oxygen at $T/T_c \cong 0.40$.

To extract the fluxoid contribution to the relaxation rates, we use fits of the data to a phenomenological form which we have shown previously to be an excellent representation of the data: $^{\eta}W_{1\alpha}/(T/T_c) = {}^{\eta}A_{\alpha}\exp[{}^{\eta}B_{\alpha}(T/T_c)]$ with $B>0$.[6] These fits to the data from Fig. 8 in the low-temperature region (i.e., below the value of T/T_c at which the strong- and weak-field data diverge) may be subtracted to yield the fluxoid contribution for both the copper and the oxygen nuclei. The fluxoid contribution for the copper, shown in Fig. 9, reveals a temperature dependence for $^{63}W_{1c}^{\text{fluxoid}}/(T/T_c) \approx (T/T_c)^{0.83}$; $^{17}W_{1c}^{\text{fluxoid}}$ is much less temperature dependent, although an exact form for the temperature dependence of $^{17}W_{1c}^{\text{fluxoid}}$ is difficult to determine due to the limited temperature range of the data (see Fig. 8).

Fluxoids can give rise to spin-lattice relaxation by several different mechanisms. Comparison of the fluxoid contributions to the copper and to the oxygen relaxation rates yields useful insight into the mechanism. We consider three possible mechanisms: (a) direct coupling of the fluxoid supercurrents to the nuclear spins combined with thermal fluctuations of the fluxoid positions, (b) relaxation of the nuclei by the conduction electrons in the cores of the fluxoids accompanied by diffusive motion of the position of the core so that all nuclei experience the core, and (c) relaxation of the nuclei by the normal electrons in the cores of the fluxoids accompanied by the exchange of energy among the nuclei via mutual spin flips between these nuclei close to the core to more distant nuclei. We label these three mechanisms as the direct relaxation, the core diffusion, and the spin-diffusion mechanisms, respectively. We take them up in turn.

(a) Direct relaxation. For this mechanism the position of the fluxoid core is merely required to vibrate. The resulting fluctuating magnetic fields permeate the sample and act directly on the nuclei. The relaxation due to these fluctuating fields would then give a rate of the forms given in Eqs. (5) and (6), or alternatively in terms of the spectral density functions[24] $k_{\alpha\alpha}(\omega)$,

$$^{63}W_{1c}^{\text{fluxoid}} = {}^{63}\gamma_n^2[k_{xx}({}^{63}\omega_0)+k_{yy}({}^{63}\omega_0)] , \tag{8}$$

$$^{17}W_{1c}^{\text{fluxoid}} = {}^{17}\gamma_n^2[k_{xx}({}^{17}\omega_0)+k_{yy}({}^{17}\omega_0)] , \tag{9}$$

where $^{\eta}\omega_0$ is the appropriate Larmor frequency. Note that the nuclear properties only enter through the $^{\eta}\gamma_n^2$ factor in front and through the nuclear precession frequency $^{\eta}\omega_0$. From study of the $^{63}Cu(2)+\frac{1}{2}\leftrightarrow-\frac{1}{2}$ and $+\frac{3}{2}\leftrightarrow+\frac{1}{2}$ transitions in the superconducting state, we know that $^{63}W_{1c}^{\text{fluxoid}}$ is to a good approximation independent of frequency. We have therefore, if this is the mechanism, essentially a white spectrum for $k_{\alpha\alpha}(\omega)$. We would then expect

$$^{63}W_{1c}^{\text{fluxoid}}/{}^{17}W_{1c}^{\text{fluxoid}} = ({}^{63}\gamma_n/{}^{17}\gamma_n)^2 = 3.82 . \tag{10}$$

However, as is shown by Fig. 10, $^{63}W_{1c}^{\text{fluxoid}}/{}^{17}W_{1c}^{\text{fluxoid}}$ ranges from 30 to 12 as T/T_c goes from 0.35 to 0.20.

Xing and Chang have recently calculated the spectral density functions $k_{\alpha\alpha}(\omega)$ for fluxoid vibrations.[33] They considered the limit of weakly damped vibrations and found that at a given temperature (1) the spectral density is not white but rather ranges form zero at $\omega=0$ to a maximum value $\omega_{\max}$ and then falls to zero as $\omega\rightarrow\infty$, (2) the frequency $\omega_{\max}$ increases with magnetic-field strength H_0, and (3) the value of $k_{\alpha\alpha}(\omega_{\max})$ is greater for smaller

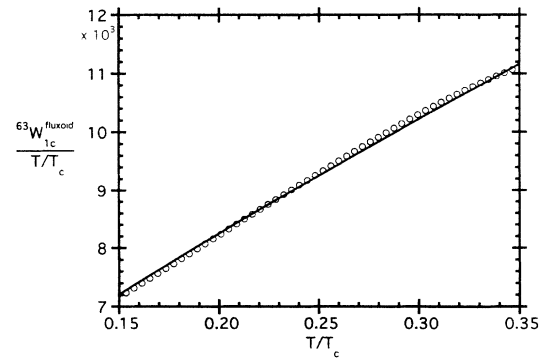

FIG. 9. The temperature dependence of the fluxoid contribution to the copper relaxation rate (circles) extracted from the experimental data of Fig. 8 (see text). The line is a fit and demonstrates that $^{63}W_{1c}^{\text{fluxoid}}/(T/T_c)$ has a temperature dependence close to $(T/T_c)^{0.83}$.

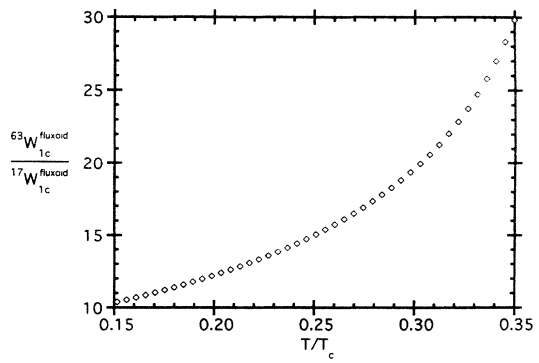

FIG. 10. The temperature dependence of the ratio of the fluxoid contribution to the relaxation rates for the copper and for the oxygen as determined from the experimental data in Fig. 8.

magnetic fields. These properties reflect the fact that in strong enough magnetic fields the fluxoids interact with each other, producing a vibration spectrum which changes with magnetic-field strength.

The calculations of Xing and Chang would not explain the white spectrum observed for the ^{63}Cu(2). Moreover, they would not give the result

$$^{63}W_{1c}^{\text{fluxoid}} \propto H_0 \tag{11}$$

found by Martindale *et al.*[7] and more recently by Ishida, Kitaoka, and Asayama[34] in $YBa_2Cu_3O_7$ and by Zheng *et al.*[35] in $YBa_2Cu_4O_8$.

We therefore conclude that direct relaxation cannot explain $^{63}W_{1c}^{\text{fluxoid}}$. It is possible that direct relaxation could explain $^{17}W_{1c}^{\text{fluxoid}}$ if there is another mechanism which is effective for ^{63}Cu(2) but not for ^{17}O(2,3). For example, spin diffusion is expected to be much faster for ^{63}Cu(2) than for ^{17}O(2,3) because the ^{63}Cu(2) nuclei have a large indirect nuclear spin-spin coupling whereas the ^{17}O(2,3) nuclei do not.

(b) Core diffusion. For this mechanism one expects that

$$^{\eta}W_{1\alpha}^{\text{fluxoid}} = f_{\alpha}(H_0)\,^{\eta}W_{1\alpha}^{\text{core}} , \tag{12}$$

where, with the field H_0 oriented along the α axis, $f_{\alpha}(H_0)$ is the fractional area of the CuO_2 planes contained in the fluxoid cores, and $^{\eta}W_{1\alpha}^{\text{core}}$ is the relaxation rate of an η nucleus which is located in a fluxoid core. Since $^{\eta}W_{1\alpha}^{\text{core}}$ should have a white spectrum, the core diffusion mechanism could explain the white spectrum observed for ^{63}Cu(2). This mechanism also satisfies Eq. (11). In Ref. 7 Martindale *et al.* showed that Eq. (12) gave a reasonable explanation of the core contribution using a core radius of 16 Å and utilizing a simple extrapolation of $^{63}W_{1c}$ just above T_c to obtain $^{63}W_{1c}^{\text{core}}$.

In $YBa_2Cu_3O_7$ the fluxoids form a lattice for $T \lesssim 75$ K.[36] This would seem to preclude the motion of fluxoids over large distances (on the order of the fluxoid lattice spacing) for the range of temperatures over which we have observed the effect of the fluxoids on the relaxation rates. This fact leads us to believe that this mechanism is unlikely as the explanation for our data.

(c) Spin diffusion. This can also explain the data if the spin-diffusion rate is fast enough. This mechanism is consistent with Eq. (11). Recent evidence also lends support to this as the mechanism responsible for $^{63}W_{1c}^{\text{fluxoid}}$.[32] As Genack and Redfield have pointed out, spin diffusion is inhibited by the field gradients one expects in type-II superconductors.[37] They derived the equations one needs to analyze the process; solution of these equations is not simple, however.

At the present time, our experiments enable us to rule out direct relaxation as the mechanism for the ^{63}Cu(2). This and the unlikely possibility that the fluxoid cores diffuse over the distances required for the size of the effect observed leads us to conclude that spin diffusion represents the most plausible explanation for the ^{63}Cu(2) data. This conclusion has been reached independently by the authors in Refs. 34 and 35.

IV. THE PAIRING STATE

The symmetry of the pairing state of $YBa_2Cu_3O_7$ is a matter of much controversy. The nature of the pairing state is important because different pairing mechanisms can yield different pairing states. Standard phonon-mediated superconductivity gives rise to a spin-singlet, orbital *s*-wave pairing state, but some spin-fluctuation models have spin-singlet, orbital *d*-wave pairing.[38] Thus, knowledge of the pairing state can aid in distinguishing between theories of the origin of superconductivity in $YBa_2Cu_3O_7$.

Analysis of the planar copper Knight shift strongly suggests that the spin pairing is singlet.[11] The Knight shift as well as the relaxation rate can also reveal information about the orbital pairing state. From such data we conclude that the orbital pairing state is not a simple isotropic *s* wave. Figure 11 demonstrates this: for a reasonably isotropic *s*-wave gap at low temperature ($T/T_c \lesssim 0.5$),

$$W_1 \propto e^{-\Delta/k_B T} . \tag{13}$$

Thus, $1/W_1$ versus T_c/T on a semilog plot should yield a straight line at low temperature with a slope given by $\Delta(0)/k_B T_c$. The data in Fig. 11 clearly do not follow this behavior. If one attempts to fit the data in the high- and low-temperature regimes to the *s*-wave exponential form of Eq. (8), one finds the high-temperature data give $\Delta(0)/k_B T_c \sim 3.1$ while the low-temperature data yield $\Delta(0)/k_B T_c \sim 0.5$.[39] For weak-coupling BCS theory, $\Delta(0)/k_B T_c = 1.75$. It is therefore apparent that at low temperatures the energy gap is effectively smaller than it is at high temperatures. The ratio of the high- to the low-temperature slopes is a factor of 6, which suggests that there is a gap anisotropy at least this big. Of course, if one assumes a *d*-wave orbital state in which the energy gap has a line of nodes, the functional dependence becomes

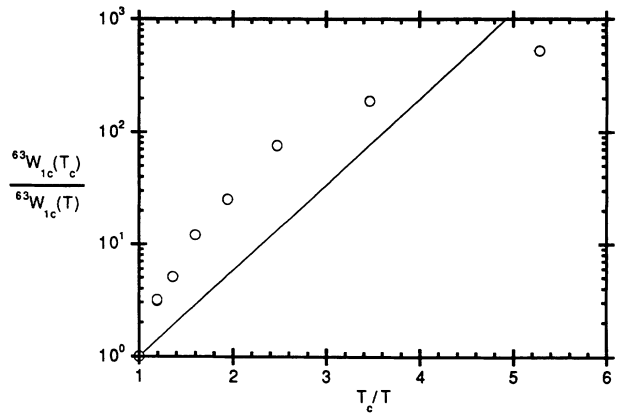

FIG. 11. $1/^{63}W_{1c}$ (measured by NQR on the same sample used for the measurements shown in Fig. 8) vs $1/T$, both normalized to their values at T_c, plotted on a semilog scale. The line is the expected temperature dependence at low temperature for spin-singlet, orbital *s*-wave pairing with an isotropic energy gap, Eq. (8), for weak-coupling BCS theory with $\Delta(0)/k_B T_c = 1.75$.

$$W_1 \propto T^3 \tag{14}$$

rather than Eq. (8). Such a law provides a reasonable fit of the data; see Fig. 12.

The arguments above to not seem to us to depend strongly on a detailed theory. They should, we suspect, be rather robust. They seem to us to rule out the conventional isotropic (or nearly isotropic) orbital *s*-wave pairing of a conventional BCS theory. We have shown previously[7,8] as have Thelen, Pines, and Lu[40] that the data can be explained quantitatively with a generalized BCS model with *d*-wave orbital pairing. A sufficiently anisotropic *s*-wave pairing state, such as has been recently proposed, may also suffice.[41]

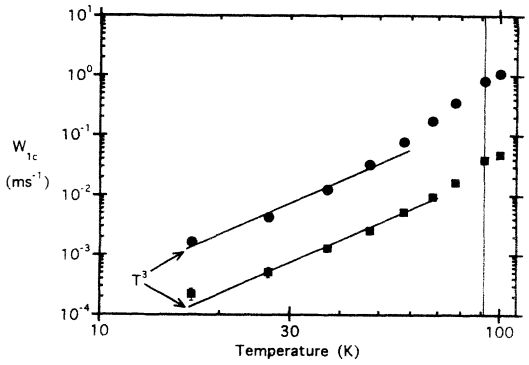

FIG. 12. W_{1c} for the ^{63}Cu(2) and ^{17}O(2,3) nuclei vs temperature on a log-log scale. The circles denote copper, and the squares denote oxygen. These data, from Fig. 8, were measured in a magnetic field strength of 0.67 T. The lines through the data indicate that both $^{63}W_{1c}$ and $^{17}W_{1c}$ have temperature dependences close to T^3 at low temperature, the result expected for some orbital *d*-wave pairing states.

ACKNOWLEDGMENTS

We gratefully acknowledge the assistance of C. Pennington, C. Klug, T. Imai, S. DeSoto, B. Corey, T. Friedmann, and J. Rice in various stages of the experiments described here as well as for many helpful discussions. We also acknowledge many useful conversations with D. Pines, J. P. Lu, D. Thelen, P. C. Hammel, L. N. Bulaevskii, I. F. Schegolev, and M. P. Maley. Two of us (S.E.B. and K.E.O.) acknowledge support from IBM and NSF, respectively. This work has been supported through the University of Illinois Frederick Seitz Materials Research Laboratory by the Department of Energy Division of Materials Research under Grant No. DEFG02-91ER45439 (J.A.M., S.E.B., D.J.D., K.E.O., and C.P.S.) and the Science and Technology Center for Superconductivity under Grant No. DMR 88-09854 (C.P.S., W.C.L., and D.M.G.).

*Also at Department of Chemistry, University of Illinois at Urbana-Champaign, 1110 West Green Street, Urbana, Illinois 61801-3080.

[1]L. C. Hebel and C. P. Slichter, Phys. Rev. **107**, 901 (1957); **113**, 1504 (1959).

[2]Y. Masuda and A. G. Redfield, Phys. Rev. **125**, 159 (1962).

[3]J. Bardeen, L. N. Cooper, and J. R. Schrieffer, Phys. Rev. **108**, 1175 (1957).

[4]D. E. MacLaughlin, in *Solid State Physics,* edited by H. Ehrenreich, F. Seitz, and D. Turnbull (Academic, New York, 1976).

[5]Z. Fisk *et al.*, Science **239**, 33 (1988).

[6]S. E. Barrett *et al.*, Phys. Rev. Lett. **66**, 108 (1991).

[7]J. A. Martindale *et al.*, Phys. Rev. Lett. **68**, 702 (1992).

[8]J. A. Martindale *et al.*, Phys. Rev. B **47**, 9155 (1993).

[9]M. E. Reeves *et al.*, Phys. Rev. B **40**, 4573 (1989).

[10]J. P. Rice, E. D. Bukowkski, and D. M. Ginsberg, J. Low Temp. Phys. **77**, 119 (1989).

[11]S. E. Barrett *et al.*, Phys. Rev. B **41**, 6283 (1990).

[12]H. Yasuoka *et al.*, Phase Trans. **15**, 183 (1989).

[13]A. J. Vega *et al.*, Phys. Rev. B **39**, 2322 (1989).

[14]Sean E. Barrett, Ph.D. thesis, University of Illinois, 1992 (unpublished).

[15]Joseph A. Martindale, Ph.D. thesis, University of Illinois, 1993 (unpublished).

[16]D. E. Farrell *et al.*, Phys. Rev. B **36**, 4025 (1987).

[17]E. L. Hahn, Phys. Rev. **80**, 580 (1950).

[18]Charles H. Pennington, Ph.D. thesis, University of Illinois, 1989 (unpublished).

[19]C. P. Slichter *et al.*, in *Pulsed Magnetic Resonance: NMR, ESR, and Optics,* edited by D. M. S. Bagguley (Oxford University Press, New York, 1992).

[20]E. R. Andrew and D. P. Tunstall, Proc. Phys. Soc. **78**, 1 (1961).

[21]A. J. Millis, H. Monien, and D. Pines, Phys. Rev. B **42**, 167 (1990).

[22]F. Borsa *et al.*, Phys. Rev. Lett. **68**, 698 (1992).

[23]M. Bankay *et al.*, Phys. Rev. B **46**, 11 228 (1992).

[24]C. P. Slichter, *Principles of Magnetic Resonance,* 3rd ed. (Springer-Verlag, New York, 1992).

[25]C. H. Pennington *et al.*, Phys. Rev. B **37**, 7944 (1988).

[26]M. Takigawa *et al.*, Phys. Rev. Lett. **63**, 1865 (1989).

[27]Y. Yoshinari *et al.*, J. Phys. Soc. Jpn. **59**, 3698 (1990).

[28]M. Horvatic *et al.*, Physica C **185-189**, 1139 (1991).

[29]M. Takigawa *et al.*, Physica C **162-64**, 853 (1989).

[30]E. Ehrenfreund, I. B. Goldberg, and M. Weger, Solid State Commun. **7**, 1333 (1969).

[31]S. M. DeSoto *et al.*, Phys. Rev. Lett. **70**, 2956 (1993).

[32]R. Corey *et al.* (unpublished).

[33]L. Xing and Y. C. Chang (private communication).

[34]K. Ishida, Y. Kitaoka, and K. Asayama, Solid State Commun. **90**, 563 (1994).

[35]G.-q. Zheng, Y. Kitaoka, K. Asayama, and Y. Kodama (unpublished).

[36]L. N. Bulaevskii and M. P. Maley (private communication).

[37]A. Z. Genack and A. G. Redfield, Phys. Rev. Lett. **31**, 1204 (1973).

[38]P. Monthoux, A. V. Balatsky, and D. Pines, Phys. Rev. Lett. **67**, 3448 (1991).

[39]C. P. Slichter *et al.*, J. Phys. Chem. Solids **54**, 1439 (1993).

[40]D. Thelen, D. Pines, and J. P. Lu, Phys. Rev. B **47**, 9151 (1993).

[41]S. Charkravarty *et al.*, Science **261**, 337 (1993).